Pacific Northwest
NATIONAL LABORATORY

PNNL-33282

Affordable Realtime Viral Detection

Demonstrated with SARS COV-2

August 2022

Samuel S. Morrison
Lance R. Hubbard
Caleb J. Allen
Amy C. Sims
Matthew J. O'Hara

U.S. DEPARTMENT OF ENERGY

Prepared for the U.S. Department of Energy
under Contract DE-AC05-76RL01830

DISCLAIMER

PACIFIC NORTHWEST NATIONAL LABORATORY
operated by
BATTELLE
for the
UNITED STATES DEPARTMENT OF ENERGY
under Contract DE-AC05-76RL01830

Printed in the United States of America

Available to DOE and DOE contractors from the Office of Scientific and Technical Information,
P.O. Box 62, Oak Ridge, TN 37831-0062
www.osti.gov
ph: (865) 576-8401
fax: (865) 576-5728
email: reports@osti.gov

Available to the public from the National Technical Information Service
5301 Shawnee Rd., Alexandria, VA 22312
ph: (800) 553-NTIS (6847)
or (703) 605-6000
email: info@ntis.gov
Online ordering: http://www.ntis.gov

PNNL-33282

Affordable Realtime Viral Detection

Demonstrated with SARS COV-2

August 2022

Samuel S. Morrison
Lance R. Hubbard
Caleb J. Allen
Amy C. Sims
Matthew J. O'Hara

Prepared for
the U.S. Department of Energy
under Contract DE-AC05-76RL01830

Pacific Northwest National Laboratory
Richland, Washington 99354

Abstract

The near real-time detection of airborne particles-of-interest is needed for avoiding current/future threats. The incorporation of imprinted particles into a micelle-based electrochemical cell produced a signal when brought into contact with particle analytes (such as SARS-COV-2), previously imprinted onto the structure. Nanoamp scales of signals were generated from what may've been individual virus-micelle interactions. The system showed selectivity when tested against similar size and morphology particles. The technology was compatible with airborne aerosol sampling techniques. Overall, the application of imprinted micelle technology could provide near real-time detection methods to a host of possible analytes of interest in the field.

Acknowledgments

This research was supported by the Strategic Investment, under the Laboratory Directed Research and Development (LDRD) Program at Pacific Northwest National Laboratory (PNNL). PNNL is a multi-program national laboratory operated for the U.S. Department of Energy (DOE) by Battelle Memorial Institute under Contract No. DE-AC05-76RL01830.

Contents

Figures

1.0 Introduction

Near real-time detection of airborne pathogens is needed to control current and avoid future pandemics [1, 2, 3, 4, 5, 6]. Described herein is a system that was developed for the near real-time detection of ambient liquid severe acute respiratory syndrome coronavirus 2 (SARS-COV-2) samples, with the demonstration of coupling to airborne sampling. The ability to detect SARS-COV-2 or other pathogens in near real time would allow rapid screening and potential early detection of virus spread. Detection methods in place include rapid antigen tests, serological surveys, and reverse transcription-polymerase chain reaction [7, 8, 9]. Currently, these methods are not compatible with airborne sampling [10, 11].
A technology compatible with airborne sampling is molecular imprinting. Imprinted technology has been shown to detect compounds of interest such as molecules, proteins, inorganic particles, viruses, and bacteria [12, 13, 14, 15, 16]. Many detection methods are optically based [15] with electronic detection methods being a less-studied aspect of the technology [16]. To advance imprinting technology to be field-deployable, we have focused on the functionalization of the imprinted technology to produce a signal that can be detected by commercial electronic systems [1, 2, 3, 4, 5, 6].
Micelles [17] in an electrochemical cell can produce measurable electronic signals when they change morphology [18, 19]. The electronic signals from the micelles can be read as changes in the properties of the bulk liquid. By incorporating the imprinting technology into a micelle, it was possible to imbue the imprinting technology with an electronic signal that can be read with commercial electronics with near real-time throughputs.
The objective of this work is to demonstrate that the integration of imprinted technology and micellular components can provide a system that allows for detection of particles or compounds of interest by commercially available electronics. Specifically, we hypothesize that:

1. The release of pmolar amounts of analyte in a sub-mL electrochemical cell can be detected by commercially available fA-scale electronics.
2. The incorporation of 100 nm scale imprinted particles at an average loading of 5-10/micelle into the outer wall of a dual-layer micelle (average diameter of 5 μm) can destabilize the micelle when brought into contact with analytes that have been imprinted on the particles.
3. Imprinted particle specificity can be applied into a biological system specifically for the detection of SARS-COV-2.

In this work, we show that the interaction between viral particles (analyte) and molecularly imprinted particles embedded into a micelle releases indicators (salts) from the micelle and generates a signal within an electrochemical cell. Please reference the graphical abstract. As this is an application involving the specific functionalization of a nanotechnology platform, care is given to ensure that the generated electronic signals originate from the analyte-indicator interaction and not from extraneous sources. To our knowledge, this is the first demonstration of airborne particulate detection with molecularly imprinted micelles. The results presented herein lend themselves to field applications and mass deployment of this sensing technology to benefit humanity.

2.0 Materials and Methods

2.1 Reagents

Ethanol (CAS: 64-17-5, 99.5%+), tetraethyl orthosilicate (TEOS, CAS: 78-10-4, 99%), ammonium chloride (CAS: 12125-02-9, 99.5%), toluene (CAS: 108-88-3, 99.5%), g-methacryloxypropyltrime-thoxysilane (MPS, CAS: 2530-85-0, 97%+), N-Isopropylacrylamide (NiPAm, CAS: 2210-25-5, 99%+), 1-(chloromethyl)-4-ethenyl-benzene (CMS, CAS: 7398-44-9, 99%), dimethyl sulfoxide (DMSO, CAS: 67-68-5,n 99%), Isopropanol (CAS: 67-63-0, 99.5%+), Azobisisobutyronitrile (AIBN, CAS: 78-67-1, 98%), diethyl ether (CAS: 60-29-7, 99.7%), 1-vinylimidazole (VIM, CAS: 1072-63-5, 99%+), phosphate buffer solution (PBS, 1.0 M pH 7.4, P3619), ammonium persulfate (APS, CAS: 7727-54-0, 98%+), N,N,N,N-tetramethylenebis(acrylamide) (TEMED, CAS: 2956-58-3, >90%), sodium chloride (NaCl, CAS: 7647-14-5, 99%+), ethylene glycol (EG, CAS: 107-21-1, 99%+), poly(ethylene glycol)-block-poly(propylene glycol)-block-poly(ethylene glycol) (PEG-PPG-PEG, CAS: 9003-11-6, 95%+), potassium ferrocyanide trihydrate (CAS: 14459-95-1, 98.5%+), octanol (CAS: 111-87-5, 99%+), linseed oil (CAS: 68553-15-1, QL 200), polyethylene glycol (PEG, CAS: 25322-68-3, 200 kDa, QL 200), gold chloride (CAS: 16961-25-4, 99.9%+), zinc chloride (CAS: 7646-85-7, 99.995%), sodium borohydride (CAS: 16940-66-2, 98%+), and sodium hydroxide (NaOH, CAS: 1310-73-2, 98%+) were purchased from Millipore Sigma or were acquired from Pacific Northwest National Laboratory (PNNL) dry storage and used without further purification.

2.1.1 Biological and Inorganic Particulate Reagents

UV light-inactivated severe acute respiratory syndrome coronavirus 2 (SARS-CoV 2) viral stocks. Under biosafety level three containment and using appropriate personal protective equipment, confluent monolayers of Vero E6 cells (from R. Baric, UNC Chapel Hill) were infected with high titer SARS-CoV 2 stock (BEI Resources NR-52284) for 35 hours at 37 °C with 5% carbon dioxide in Minimal Essential Media (Gibco 11095080) containing 4% fetal bovine serum (Cytiva Hyclone SH3007003HI) and 1X antibiotic/antimycotic (Gibco 15240112). As part of the natural infection cycle, infectious SARS-CoV 2 is released into the media on top of infected cells. Supernatant (media) from infected cells was collected and gently centrifuged (Sorvall Legend Biocontainment rotor at 500xg for 5 minutes) to remove cellular debris. Supernatant (in 1mL aliquots) was added to each well in a six-well plate (Corning 3506) and exposed to UV treatment for 10 minutes. The plate was rotated 180° and the UV treatment was repeated to inactivate SARS-CoV 2 virions. Following treatment, the inactivated virus was collected into 2 mL free standing o-ringed tubes and frozen at -80 °C. The UV treatment was repeated until all the media from the infected flask had been inactivated. The UV lamp (UVP 95-0007-06 Model UVGL-58 6-watt UV lamp) used was brand new and was ~11.43 cm from the six-well plate. We estimate the dose to be ~1462 mJ/cm^2 at 254 nm. UV-inactivated media was evaluated by plaque assay to confirm all replication-competent SARS-CoV 2 virions were rendered no longer infectious. Vero E6 cells were plated in six-well plates and serial dilutions of UV-treated and non-treated SARS-CoV 2 samples in 1X sterile Dulbecco's phosphate buffered saline (Gibco 14190250) were added to the appropriate wells and covered with Dulbecco's minimal essential media (Gibco 11965092), 4% fetal bovine serum, 1X antibiotic/antimycotic, and 0.8% low melting point agarose (Lonza SeaKem LE Agarose 50002). Plaque assay plates were assessed 72 hours post-infection with 1X neutral red stain (Invitrogen N3246). Following Institutional Biosafety Committee approval of the UV inactivation protocol, samples were removed to biosafety level two for further studies.

2.1.2 SARS-CoV 2 spike pseudotyped particles

Bacterial plasmid constructs containing fragments of the lentiviral vector and SARS-CoV 2 spike gene were transformed into chemically competent *E. coli* (TOP10 Invitrogen C404003) using heat shock; plasmid confirmation was performed by restriction enzyme digestion screening; selected clones were grown in liquid media cultures under antibiotic selection; and plasmid extraction was performed using a Qiagen miniprep kit (Qiagen 27106) according to the manufacturer's instructions. Under biosafety level two conditions, human embryonic kidney 293T cells expressing the human angiotensin converting enzyme 2 (ACE2 protein, SARS-CoV 2 receptor BEI Resources NR-52511) were expanded and plated in Dulbecco's minimal essential media (Gibco 11965092) supplemented with 10% fetal bovine serum

(Cytiva Hyclone SH3007003HI), 2mM L-glutamine (Gibco 25030081) and 1X penicillin streptomycin (Gibco 10378016; D10 growth media) at 5x10^5 cells per well for a six-well plate. Between 16 and 24 hours post-plating, 7.5 mL lipofectamine 3000 (Invitrogen L3000015) in 125 mL Opti-MEM I media (Gibco 31985070) was mixed with plasmid DNA (1mg lentivirus backbone/luciferase/green fluorescent protein (BEI Resources NR-52516), 0.34 mg spike glycoprotein (BEI Resources NR-52514), 0.22 mg helper Rev1b (BEI Resources NR-52519), 0.22 mg helper Tat1b (BEI Resources NR-52518), 0.22 mg helper Gag/Pol (BEI Resources NR-52517) in 125 mL Opti-MEM I media with 5 mL P3000 reagent (provided with the lipofectamine 3000) per well and used to rescue SARS-CoV 2 pseudotyped particles. The following morning, the DMEM plus transfection reagent and DNA was removed and 2 mL D10 growth media was added. Media were harvested from the transfected cells at 60 hours post-transfection and filtered through 0.45 mM surfactant free cellulose acetate (SFCA) low protein binding filter (Corning 431220) prior to storage at -80 °C. Human coronavirus NL63 stock: LLCMK2 cells (non-human primate kidney cells from Ralph Baric's laboratory UNC Chapel Hill) were grown to 80% confluence and inoculated with 500 µL clinical isolate of human coronavirus NL63 (HCoV-NL63) obtained from BEI Resources (NR-470) and incubated at 32 °C until half of cells were involved in cytopathic effect. Supernatant was removed from the infected cells, gently pelleted at 500xg for 5 minutes to remove cellular debris, aliquoted and frozen at –80 °C until tested [23]. Rabbit anti-guinea pig IgG whole molecule antibodies polyclonal secondary antibody (Abnova Corporation PAB9253) and luminescent particular tracers for fluorescent video imaging were collected from stores of [24] and functionalized with ascorbic acid (Vit.-C, CAS: 50-81-7, 99%) by ligand exchange [25].

2.1.3 Sensitized Micelle Synthesis

Prior to incorporation into the outer micelle wall, the functionalized silica spheres were prepared similarly to [15] as follows, as depicted in, Fig. 1.

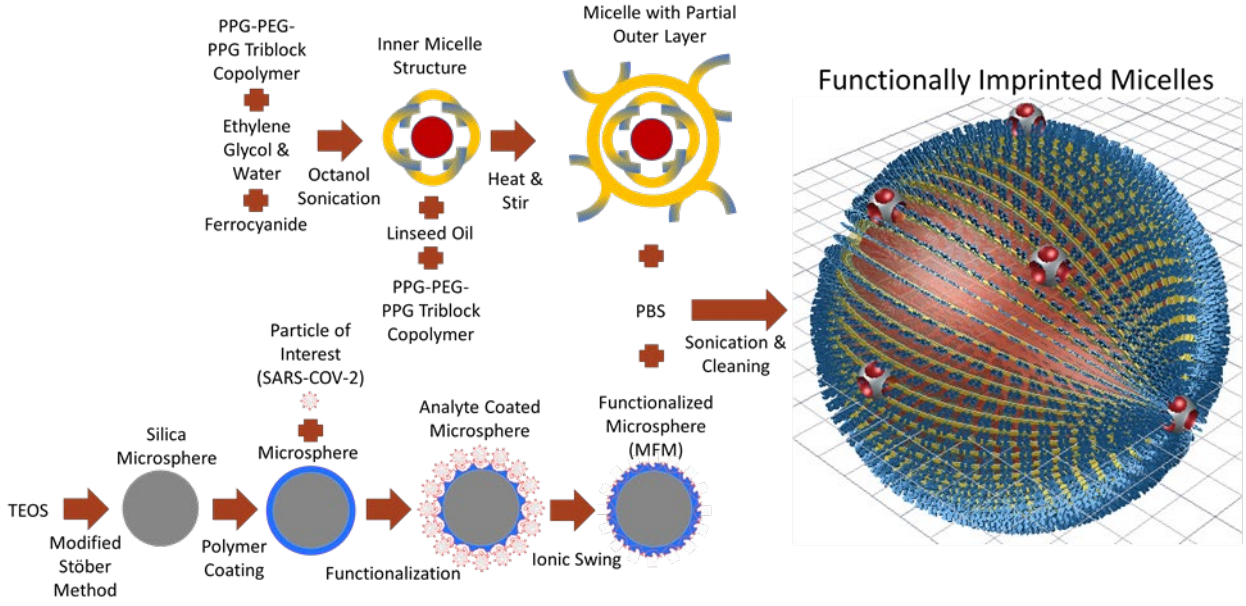

Fig. 1 Displayed is the scheme for visualization of the synthesis steps and reaction for the functionally imprinted micelles.

Silica Sphere Synthesis. 45.5 mL of ethanol and 4.5 mL of TEOS were mixed in ambient environment after which a solution of 16.2 mL of ethanol, 26.3 mL of deionized water (DIW), and 7.5 mL of ammonium chloride were added. The solution was vigorously stirred at 10 °C and incubated for 2 hours. Then, 150 mL of toluene was added and 1 mL of MPS was added under argon and stirred for 48 hours at 50 °C. The particles were centrifuged (7000 rpm) and washed separately in ethanol, DIW, and toluene. Lastly, the particles were dried under vacuum at 60 °C for 24 hours and stored under argon.

Macromolecularly Functional Monomers (MFMs). In a 25 mL flask a stir bar, 2.26 g of NiPAm, and 1.02 g of CMS were added. The powders were dissolved in 8 mL of 50 vol% DMSO and isopropanol.

Then 3 mg of AIBN were added to the solution, which was deoxygenated by argon purge for 1 hour at ambient temperature. The solution was then heated to 75 °C for 8 hours. The MFMs were precipitated by addition of 50 mL of freezing diethyl ether. The solid was dissolved in 10 mL of DMSO and 0.63 g of VIM was added dropwise at 50 °C. The solution was stirred for 8 hours at 50 °C and then the solids were precipitated with freezing diethyl ether and washed with 100 mL of ether. Lastly, the solid MFMs were dissolved in 5 mL of DIW.

2.1.4 Particle Imprinting of MFM-Silica and Gold-PEG particles (IMPs)

2.1.4.1 Biology

0.2 mg of the particle to be tested were suspended in 50 mL of PBS to which 20 mg of MFM was added. The suspension was incubated at 30 °C for 3 hours. The liquid was degassed under vacuum for 10 min and then purged with argon for 10 min. To the liquid 4 µL of APS and 2 µL of TEMED were added and stirred violently at 30 °C 24 hours. The particles were collected by centrifugation (7000 rpm, 1 hour) and washed separately with DIW and then 0.5 M NaCl solution. The resultant suspension was stored in 0.5 mL of DIW under argon at 5 °C.

2.1.4.2 Biology (Virus-like Pseudo-particles and Inactivated Virions)

Pseudo-particles with SARS-CoV 2 spike proteins or UV-inactivated SARS-CoV 2 stocks (~1 mL) were suspended in 2.5 mL of PBS to which 5 mg SiO_2 and 1 mg of MFM were added. The suspension was incubated at 30 °C for 3 hours with vigorous stirring. To the liquid 10 µL of 0.2% w/v APS and 10 µL of 0.1% v/v TEMED were added and stirred violently at 30 °C for 12 hours. The particles were collected by centrifugation (1750xg, 20 minutes) and washed separately with DIW, 0.5 M NaCl solution, and a final DIW wash. The resultant suspension was stored in 0.5 mL of DIW in a glass vial until added to the SM solution as described below.

2.1.4.3 Inorganic

To make the imprinted Au-PEG particles, 100 mg of PEG 200k Da, was added to 20 mL PBS. This was stirred on high for 10 min to dissolve. 5 mg of 300 Da PEG was added followed by 5 mg of the desired analyte particle. 20 mg of gold chloride was added to the beaker. 10 mg of sodium borohydride was then added (carefully) to the solution. The solution, a pale yellow from the gold, was heated to 30 °C and slowly stirred. Small black flecks formed in the liquid after 5 minutes. After 1.5 hours, the solution turned a gray-yellow color. After an additional hour, 50 mg of zinc chloride was added, and it was cooled to room temperature. This was centrifuged (7000 rpm) for 30 minutes and the solution decanted off. The remaining solid was put in 5 mL of PBS to make the PEG-AuNP lock solution

2.1.5 Inner Micelle Structure (IMS)

10 ml of EG and 10 ml of DIW were added to a beaker to which 180 mg of PEG-PPG-PEG was added. The solution was stirred at 500 rpm for 1 min, to which 5 mg of potassium ferrocyanide trihydrate was added. 5 more mL of DIW were added and the suspension was stirred at 80 °C for 10 min at 500 rpm. 7.5 mL of the IMS suspension was added to 20 mL of octanol and sonicated for 30 min (40 kHZ, 40 W). Then it was spun in a centrifuge at 7000 rpm for 2 hours until the three layers were observed. The top layer was octanol slightly cloudy with micelles, the middle layer was murky, and the bottom layer was water. The top layer was decanted and collected to finish the first micelle wall solution.

2.1.6 Incorporation of MFM-Silica into Outer Wall of Sensitized Micelles

20 mL of linseed oil and 325 mg of PEG-PPG-PEG were stirred vigorously for 10 min at 60°°C (in biological safety cabinet [BSC] 80 °C for 20 min or until dissolved). 20 mL of the IMS suspension was added and stirred vigorously (1500 rpm) for 10 min at 60 °C (in BSC 80 °C for 5 minutes or until dissolved). 200 µL of the IMPs suspension (500 µL of biological IMPs) were added to the oil suspension and stirred vigorously for 5 more min at the same temperature. The micellular suspension was removed from heat (in the BSC, the heat block temperature was reduced to 40° C) and stirred at 1500 rpm for 5 more min. Lastly, to the suspension 50 mL of basic DIW (200 mg NaCl, 50 mg NaOH) was added and stirred at 40 °C for 5 min, then sonicated (BSC in an ice bath) (40 kHz. 40 W) for 60 min. The suspension

was centrifuged at 700 rpm for 3 hours (1750xg for a total of 2 hours) stopping each hour to remove oil from the top of the suspension. Lastly, the now suspension of SMs was stored under ambient conditions (4°C for biological material) in the water mixture until needed for measurement.

2.2 Experimental Methods

2.2.1 Electrochemical Cell

The electrochemical testing of the SMs was performed in a 100 µL glass vial with an outer polystyrene shell (The Lab Depot Inc., Catalogue Code: 30111G-1232). Two platinum wires (5% Mo, 50 µm dia.) were inserted into the vial and separated by a small piece of PTFE. 100 µL of DIW (cleaned at 2V for 48 hours) was injected into the vial and held at the analysis voltage from 15 min to remove any remaining electrolytes in the bath. When the experimental measurements were run, 5 µL of the micelle solution was injected into the cleaned water, as well 5 µL of the desired analyte solution.

The cell was held in a rubber-covered steel clamp that completely covered the cell. The clamp provided mechanical stability and radio frequency shielding. The metal platform of the cell was grounded to the electrometer and rested on two 3 mm thick sheets of PTFE plastic for electrical isolation. Several layers of alumina-silicate mat were placed under the PTFE, which isolated the cell from common laboratory vibrations and the ventilation vibration inherent in biological-rated hoods.

The electrical bias and measurement were performed by a high-resistance electrometer (Keysight Inc., B2985A). Tri-ax cabling (Pamona Inc., Model number: 4725) was used to connect the cell and electrometer. The ground of the electrometer was used for all grounding shield lines so that the cell and electrometer were at the same electrical bias. The electrometer was isolated vibrationally using a rubber mat. The electrometer applied from -0.25 to -0.8 V (typically -0.25 V was used) based on cyclic voltammetry (Fig. S3) performed on the SMs. The electrometer was set from 100 to 100k samples/s depending on the experiment. Common noise levels achieved in the cell were from 15 to 150 pA, depending on supply-side line noise.

2.2.2 Photoluminescent Video

Luminescent video was taken on a OMAX EPI-2500X fluoromicroscope under 100 W of broadband UV irradiation. Addition of analytes to a 20 µL drop of micelles on a glass slide was imaged in the microscope and video was taken from 10-0.5 frames/s.

2.2.3 Airborne Particle Sampling and Condensation

The aerosol condensation setup was constructed of standard laboratory glassware (see Fig.3a and b). One system inlet allowed for the analyte particle input, the other for the generated aqueous aerosol fog (AGPtek, 100W, 20 kHz) to bind with the air particles. The fog was generated from deionized water >17.8MOhm. A shared nitrogen gas valve (1-10 L/min STP) was used to create the air flow throughout the system, carrying both the input analyte particle sample and the particle-collecting fog. Low air flow was used, allowing just enough flow to begin visually generating a vortexing behavior where the two inputs mixed at a three-way adapter glassware. The gas flow then traveled through a sloped condenser glassware, through which a pumped refrigerant at 0 °C flowed through the outer vessel of the condenser. This encouraged the condensation of the fog with the aerosol particle, leading to a two-neck round bottom flask where the sample was collected. This flask is also submerged in an ice bath to help encourage any final condensation of the carrier fog. The second neck of the flask is an outlet to a secondary collection bottle filled with quartz wool to collect remaining fog not condensed. This setup has been measured to collect approximately 0.45 g/min. of condensed fog.

2.3 Data Analysis

A Python script was created to automate the data processing, a copy of the code is recorded in the supplementary information. The raw current and time data were parsed from the electrode and corrected to center around zero. From the noisiest background, taken from the determining the largest standard deviation, the maximum and minimum signals were taken. From the sample count data, the region between the maximum and minimum was removed. The resulting absolute value of the data was then plotted.

3.0 Results

To test the release of the indicator and confirm the electronic signal generated from the release: Fig. 2 demonstrates the micelle-analyte interaction optically and electronically. Fig. 2 a-c shows the micelles frame-by-frame as the analyte diffuses from left to right in the photoluminescent video stills, a cartoon depiction of the association of an analyte particle releasing materials from the micelle is included as the graphical abstract. The micelles are seen to “pop” as they lose their luminescent mid-layer (the linseed oil). As micellular ions are released into the bath, the minute changes in resistivity are registered as an electronic signal, which is exemplified in Fig. 2d and for longer time scales in Fig. S1.
Fig. 2d shows the resultant electronic signals resulting from serial dilutions of analyte particles. A suspension of 2.5 ng of analyte particles (1X in the image legend, 5 µL of a 500 ng/mL suspension) was injected and evaluated. Subsequent dilutions of 10X were also evaluated for their electronic response. The results are visible in the graph until the 10kX dilution was evaluated (250 fg). Subsequent data analysis resulted in isolated single micelle-analyte reactions being recorded by further diluted samples. Fig. 2e gives an overview of the results from five trials at sub-fg amounts of analyte (between 50 and 500 viruses/injection). As can be seen in Fig. 2e, after an initial mixing period, the system returned about 25 discrete sensitized micelle (SM) -analyte events.

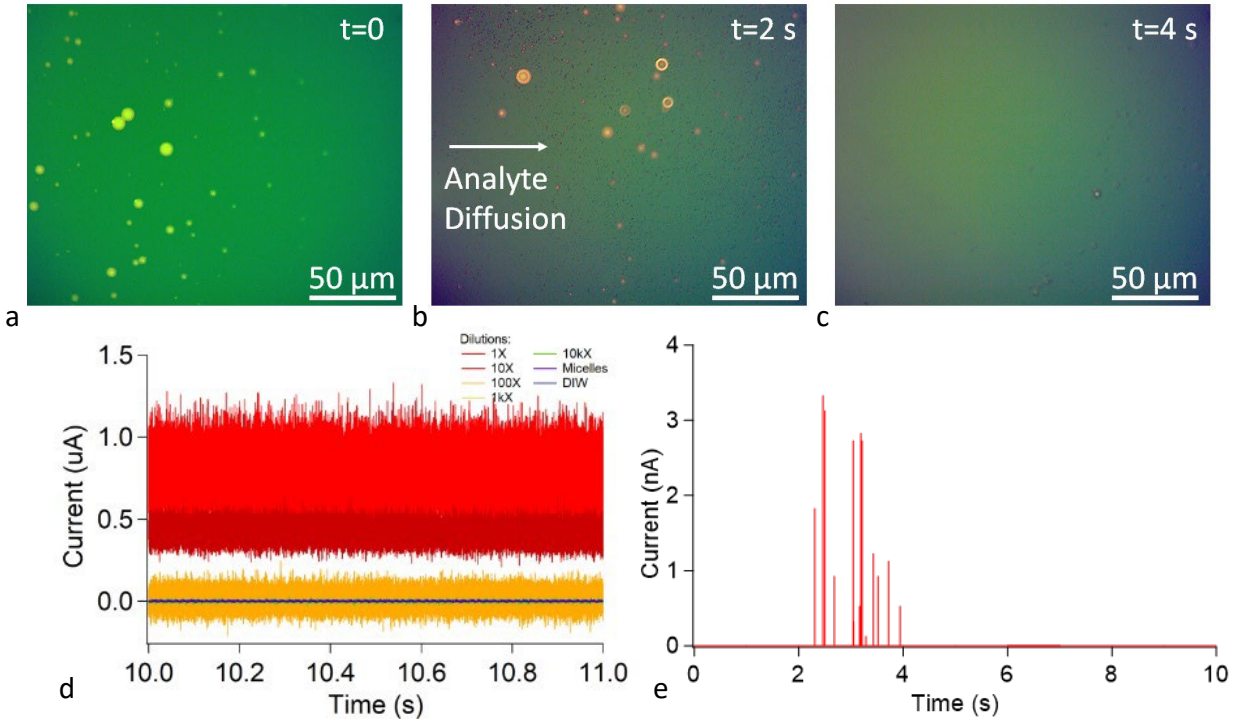

Fig. 2 a) Fluoromicrograph of the micelles floating in suspension at the time of analyte introduction to the liquid (out of frame). b) Fluoromicrograph of the micelles as the analyte diffuses into the micelle suspension. The release ion exchange appears as concentric rings of luminescence. c) The resultant liquid suspension of micelles after mixing with the analyte. Few micelles are seen. d) The electronic signal as a function of serial dilutions of analyte particles. e) The electronic signal after 2 sigma background elimination of very dilute >pg/ml analyte samples

With a high degree of sensitivity established, the electronic response relative to many controls was evaluated to make sure that the measured signal originated from SM-analyte interaction (Fig. 3a and b). As seen in Fig. 3b, the micelle-analyte interactions produce significantly more signal than control measures. To ensure that the signals seen were not generated by noise on the power supply line, the frequency distribution was established (Fig. 3c). As can be seen, there is a stochastic aspect to the signal as expected from Brownian motion of diffusion.

As the sensitivity and SM-analyte interaction aspects of the signal were established, the selectivity of the SMs was then evaluated. Fig. 3d shows the normalized response and signal width (error bars, blue line) of SAR-COV-2 imprinted micelles tested again other analytes. The total integrated response of each analyte is also presented (red line). As can be seen in Fig. 3d, the signal is diminished significantly when other analytes are tested. Most notably, the SM system could see a difference between pseudo particles of SARS-COV-2, active virus HCoV-NL63, and ultraviolet (UV)-inactive SARS-COV-2. While HCoV-NL63 did, in some instances, produce event magnitudes in line with the size of the SM-SARS-COV-2 interactions, the total integrated response was very diminished.

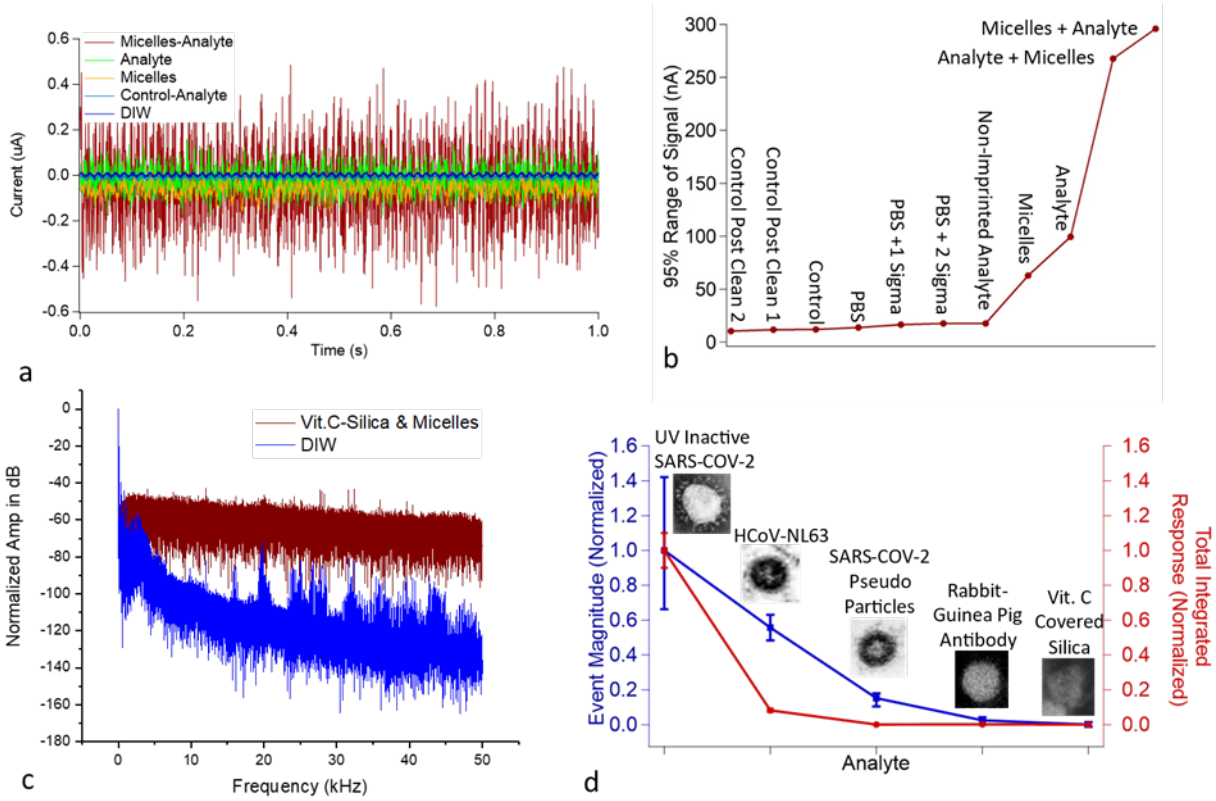

Fig. 3 a) The electronic signal of the micelle-analyte interaction versus time and compared to various backgrounds. b) The magnitude of the electronic signal of the micelle-analyte interaction versus a large number of controls. c) The fast-Fourier-transform of the micelle-analyte interaction versus a control to demonstrate the stochastic nature of the interactions. d) The relative specificity of the micelle-analyte interaction to similar particles in both event magnitude and total response. The inlays are transmission electron microscopy (TEM) images of each type of particle

As the sensitivity and selectivity of the SM system has been established, the next step was to design an airborne particle collection system which can integrate with the SM electrochemical cell. Initial airborne detection of analyte particles was accomplished, and an overview is presented in Fig. 4. Fig. 4a is a macro image showing vortex mixing of the sampled ambient air containing analyte particles and mixing with a generated aqueous aerosol. In this manner, the particles from the air are transitioned from suspension in air to suspension in water particles [20, 21, 22]. Fig. 4b depicts the flow of the aerosol as it is condensed into a single liquid water volume and then stored at 0 °C (prior to testing in the electrochemical cell). Fig. 4c shows the high-resolution data of the cell response with an aliquot of the analyte particles that had been condensed into the liquid water. Lastly, Fig. 4d shows a longer time measurement to gain an understanding of how long analyte particles generate a response when injected into the SM cell.

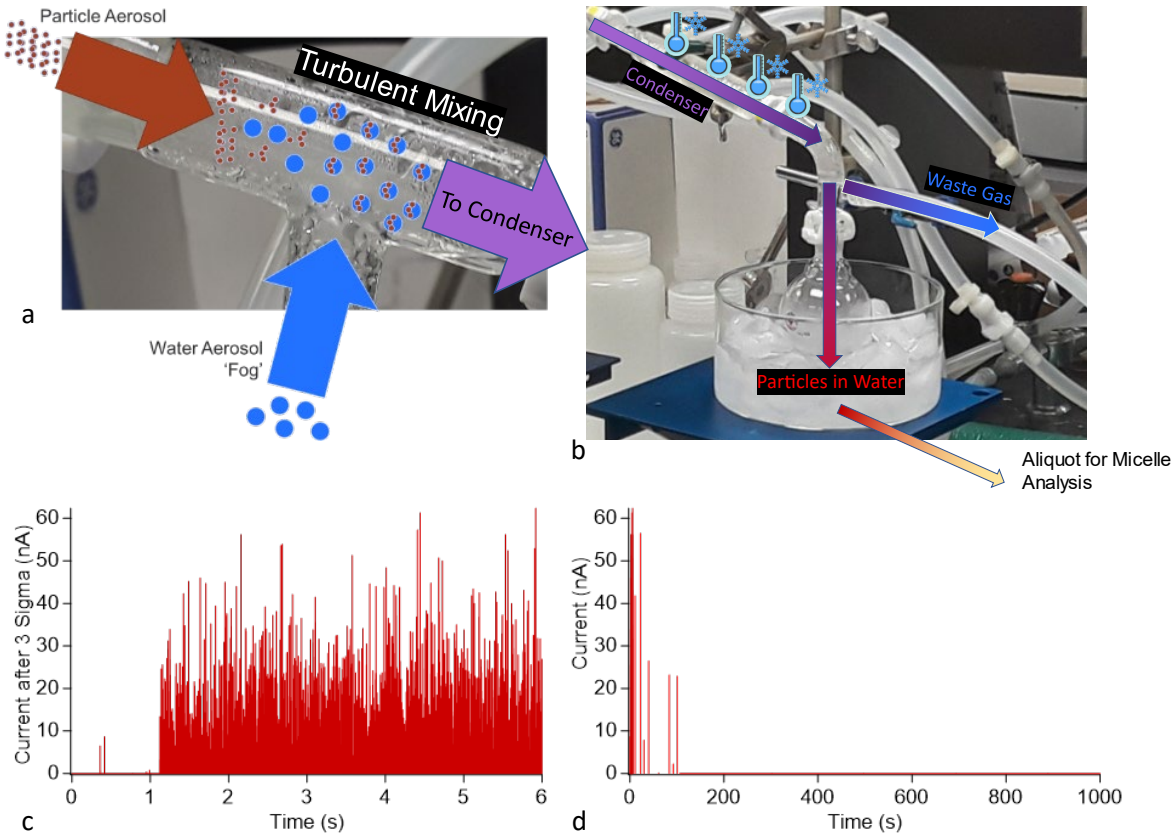

Fig. 4 a) Image of the sampling chamber where ambient air is mixed with generated aqueous aerosols. The relative flow of analyte particles is overlayed on the image. b) Image of the condensation chamber where the analyte-filled aerosol is captured in liquid water while carrier gas and air are removed from the system. An arrow shows that samples are taken from the liquid and injected into the electrochemical detection cell. c) The near-time electrochemical results showing a preliminary mixing phase followed by strong signal as the analyte liquid is introduced into the cell. d) The longer-time life of the analyte-micelle signal

4.0 Discussion

The initial hypothesis detailing the electronic detection of pmol levels of analyte into a sub-mL bath is supported by the results of Fig. 2. The sensitivity of the system and what appear to be SM-analyte interaction at the pg/mL levels of analyte show that the imprinted micelle technology can generate signals from pmolar levels and perhaps smaller.

The secondary hypothesis that revolves around the functionalization of micelles with imprinted particles is supported by the many backgrounds and control evaluations in Fig. 3. The micelles appear to respond to the presence of imprinted analytes with a degree of specificity, resulting in a larger electronic signal than background evaluation or the presence of particles not imprinted on the micelle.

As demonstrated by the results in Fig. 4, the electrochemical SM cell is compatible with biological aerosol sampling methods. The combination of the cell results from Fig. 2, Fig. 3, and Fig. 4 suggest that it is possible to integrate the use of imprinted SMs, commercial electronics, a nd established bioaerosol sampling methods to real-time field-based detection of analyte particles of interest. We have demonstrated this detection for two specific inorganic and viral particles.

5.0 Conclusion

Electronic signals have been generated from functionalized micelles, imprinted to specific analytes of interest. The ability to detect analytes of interest such as SARS-COV-2 with a system that can be adapted for field use allows for wide-scale deployment of imprinting technology. The technology could be used for industrial pollutant detection, viral emissions in buildings, the presence and growth of bacterial species in foods, and many other applications involving the detection of compounds in an ambient setting.

6.0 References

1. J. Shin, H.R. Kim, P.K. Bae, H. Yoo, J. Kim, Y. Choi, Scientific Reports. (2021) https://doi.org/10.1038/s41598-021-98207-1

2. J. Ma, G. Jiang, Q Ma, H Wang, M Du, C Wang, X Xie, Analyst. (2022) https://doi.org/10.1039/D1AN02104D

3. C. Park, J. Lee, D. Lee, J. Jang, Sensors and Actuators B: Chemical. (2022) https://doi.org/10.1016/j.snb.2021.131321

4. R.R. Kalavakonda, M.V.R. Masna, S. Mandal, S. Bhunia, Scientific Reports. (2021) https://doi.org/10.1038/s41598-021-99150-x

5. J. Bhardwaj, S. Hong, J. Jang, C.H. Han, J. Lee, Elsevier. (2021) https://doi.org/10.1016/j.jhazmat.2021.126574

6. I. Lee, Y Seok, H Jung, B Yang, J. Lee, J. Kim, ACS Publications (2020) https://doi.org/10.1021/acssensors.0c01531

7. A. Kruttgen, C.G. Cornelissen, M. Dreher, Journal of Virological. (2021) https://doi.org/10.1016/j.jviromet.2020.114024

8. J. Lourenco, R. Paton, C. Thompson, P. Klenerman, MedRxiv. (2020) https://doi.org/10.1101/2020.03.24.20042291

9. S. Jeong, E. Gonzalez-Grandio, N. Navarro, R.L. Pinals, ACS Publications. (2021) https://doi.org/10.1021/acsnano.1c02494

10. P. Moitra, M. Alafeef, K. Dighe, P. Ray, Biotechnology and Bioengineering. (2021) https://doi.org/10.1002/bit.27812

11. N. Kumar, N.P. Shetti, S. Jagannath, T.M. Aminabhavi, Chem. Eng. J. (2022) https://doi.org/10.1016/j.cej.2021.132966

12. R. Ahmad, N. Griffete, A. Lamouri, N. Felidj, M.M. Chehimi, C. Mangeney, Chem. Mater. (2015) https://doi.org/10.1021/acs.chemmater.5b00138

13. L. Chen, X. Wang, W. Lu, X. Wu, J. Li, Chem. Soc. Rev. (2016) https://doi.org/10.1039/c6cs00061d

14. M. Niu, C. Pham-Huy, H. He, Microchim. Acta (2016) https://doi.org/10.1007/s00604-016-1930-4

15. L. Qian, X. Hu, P. Guan, D. Wang, J. Li, C. Du, R. Song, C. Wang, W. Song, Anal. Chimica Acta (2015) https://doi.org/10.1016/j.aca.2015.05.015

16. Y. Saylan, F. Yilmaz, E. Özgür, A. Derazshamshir, H. Yavuz, A. Denizli, Sensors (2017) https://doi.org/10.3390/s17040898

17. R. K. O'Reilly, C.J. Hawker, K.L. Wooley, Chem. Soc. Rev. (2006) https://doi.org/10.1039/b514858h

18. V. C. Ferreira, A. F. Silva, L. M. Abrantes, (2010). https://doi.org/10.1021/jp912123m

19. M. Macka, W. C. Yang, P. Zakaria, A. Shitangkoon, E. F. Hilder, P. Andersson, P. Nesterenko, P. R. Haddad, J. Chromatogr. A (2004) https://doi.org/10.1016/j.chroma.2004.03.074

20. J. Cox, H. Mbareche, W. G. Lindsley, C. Duchaine, Aerosol Sci. Technol. (2020) https://doi.org/10.1080/02786826.2019.1688759

21. Y. Liu, Z. Ning, Y. Chen, M. Guo, Y. Liu, N.K. Gali, L. Sun, Y. Duan, J. Cai, D. Westerdahl, X. Liu, K. Xu, K. Ho, H. Kan, Q. Fu, K. Lan. Nature (2020) https://doi.org/10.1038/s41586-020-2271-3

22. N. Riemer, A. Ault, M. West, R. Craig, J. Curtis, Rev. Geophys. (2019) https://doi.org/10.1029/2018RG000615

23. E.F. Donaldson, B. Yount, A. C. Sims, S. Burkett, R. J. Pickles, R. S. Baric, J. Virol. (2008) https://doi.org/10.1128/JVI.01804-08

24. L. Hubbard, R. Sumner, M. Liezers, T. Cell, C. Reed, N. Uhnak, C. Allen, B. Berry, H. Currah, E. Fuller, E. Kinney, N. Smith, M. Foxe, A. Carman, Rugged nanoparticle tracers for mass tracking in explosive events. MRS Commun. (2020) https://doi.org/10.1557/mrc.2020.70

25. M. J. Choi, L. K. Sagar, B. Sun, M. Biondi, S. Lee, A. M. Najjariyan, L. Levina, F.P. Garcia de Arquer, E.H. Sargent, Nano. Lett. (2021). https://doi.org/10.1021/acs.nanolett.1c01286

Pacific Northwest National Laboratory

902 Battelle Boulevard
P.O. Box 999
Richland, WA 99354

1-888-375-PNNL (7665)

www.pnnl.gov